Angewandte Chemie
Eine Zeitschrift der Gesellschaft Deutscher Chemiker

Supporting Information

Dual-Function HKUST-1: Templating and Catalyzing Formation of Graphitic Carbon Nitride Quantum Dots Under Mild Conditions

Mohamed K. Albolkany, Yang Wang, Weijin Li, Syeda Arooj, Chun-Hui Chen, Niannian Wu, Yan Wang, Radek Zbořil, Roland A. Fischer, and Bo Liu**

anie_202009710_sm_miscellaneous_information.pdf

1. Experimental Section

1.1. Chemicals:

Copper nitrate trihydrate, ethanol, dichloromethane, hydrochloric acid, and nitric acid were purchased from Sinopharm chemical reagent Co., Ltd (Shanghai, China), copper acetate monohydrate was ordered from Shanghai Macklin Biochemical Co., Ltd. 1,3,5-benzene tricarboxylic acid (H_3BTC) was bought from Aladin Chemicals Co. Cyanamide (CA) was acquired from Energy Chemicals Company.

1.2. HKUST-1 preparation and activation:

HKUST-1 was prepared according to the previous report[1] as follows:

0.435 g of $Cu(NO_3)_2.3H_2O$ (1.8 mmol) was dissolved in 6 ml DI water (solution A) and 0.21 g H_3BTC (1 mmol) was dissolved in 6 ml ethanol (solution B). Then, the two solutions were mixed and kept under stirring for 30 min. The mixture was heated in Teflon lined stainless steel autoclave for 12h at 120 ^oC. After cooling down, HKUST-1 crystals were collected and washed with ethanol: water (1:1) several times followed by washing with ethanol 3 times and dried in oven at 80 ^oC for 12 h.

MOF crystals were activated by soaking in dichloromethane (DCM) for 12 h.[2] During this period DCM was replaced with fresh one 5 times to completely exchange water and ethanol attached to the active sites.

The dark blue crystals were obtained under dynamic vacuum at 150 ^oC for 12 h before using it for g-CNQDs formation.

1.3. g-CNQDs@HKUST-1 preparation:

Loading and catalytic polycondensation of CA were done sequentially in HKUST-1 pores as follows: In a typical procedure, 0.6 g activated HKUST-1 was loaded in homemade cylindrical porous aluminum holder (3 cm x 1 cm) in nitrogen atmosphere. The sample holder was fixed at 1 cm height above 1 g of CA powder in 20 ml glass vial closed with silicone plug, which was then evacuated for 30 min followed by heating in stainless steel protective jacket in oven (temperature programming: temperature increased from room temperature to 80 ^oC during 1 h then kept at 80 ^oC for 6 h followed by another increase to 120 ^oC within 1h. Heating at the

polycondensation temperature was continued for 15 h, then the sample was cooled down naturally to room temperature).

The counter experiment using anhydrous copper acetate and copper nitrate was done under the same conditions like g-CNQDs formation except that, the copper forms were directly mixed with cyanamide at the bottom of the glass vial (0.15 g copper salt + 0.5 g CA). We skipped the loading step (used in case of HKUST-1) as these copper salts are non-porous. After cooling down to room temperature, the products were washed with HCl (1 M) several times then HNO_3 (2 M) to completely remove the copper ions and counter anions (acetate or nitrate). The pale yellow products were washed with DI water (5 times) then dried under vacuum at 110 ºC/12 h.

1.4. g-CNQDs extraction and cleanup:

For further characterization, g-CNQDs (prepared at 120 ºC/15 h) were extracted from the MOF pores by etching the framework in acidic medium (1M HCl) and removing the ligand by extraction with diethyl ether. The acidic aqueous solution was dialyzed against DI water for 3 days using regenerated cellulose bags (RC-1000 Da). Pure g-CNQDs were sonicated in 2 M HNO_3 for 2 h to completely remove the copper ions attached on the surface. The acidic yellow solution was dialyzed again against DI water till neutralization.

1.5. Characterization instruments:

Fourier transform infrared (FT-IR) spectra were collected by SHIMADZU IR Affinity-1 spectrometer using KBr discs in the range from 4000 to 400 cm^{-1}. Elemental analyses (EA) were carried out on Vario EL III Elemental Analyzer (Elementar Inc.). Powder X-ray diffraction (PXRD) measurements were done using Rigaku MiniFlex 600 X-ray diffractometer with Cu Kα radiation (λ = 1.54178 Å). Thermogravimetric analyses (TGA) were done in the range from 25 to 800 ºC in N_2 atmosphere. The heating rate was 10 ºC/min using TGA Q5000 IR thermal analyzer. N_2 sorption isotherm was measured on a BELsorp-max machine, BEL, Japan at 77 K. Samples had been activated at 120 ºC for 12 h under mechanical vacuum before N_2 sorption measurements. Scanning electron microscopy was carried out with a field-emission scanning electron microanalyzer (GeminiSEM 500). Nuclear magnetic resonance (NMR) spectra were recorded on a Bruker AVANCE III HD spectrometer operating at 400 MHz. X-ray photoelectron spectroscopy (XPS) analysis was done on an ESCALab 250 high-performance electron

spectrometer using monochromatized Al Kα radiation (hν = 1486.7 eV) as the excitation source. Transmission electron microscopy (TEM) was conducted using Jeol JEM-2011 TEM with an accelerating voltage of 200 kV. Atomic force microscopy images (AFM) were recorded using a tapping mode AFM (Asylum Research MFP-3D AFM). UV-Vis spectra of g-CNQDs were collected using TU-1810 UV/Vis spectrophotometer (Beijing Pgeneral, China) and photoluminescence (PL) was measured on Hitachi fluorescence spectrophotometer (F-4600). The g-CNQDs surface charger was measured using zeta potential meter (NanoBrook 90Plus PALS).

Table S1. Carbon and nitrogen percentage in the composites after loading cyanamide at 80 ºC for 6 h and polycondensation at different temperature degrees for 15 h.

Steps	**C %[a]**	**N %**	**C/N ratio**
Step 1: Loading at 80 ºC	1.83	3.69	0.50
Step 2: Polycondensation at:			
90 ºC	4.82	10.10	0.48
120 ºC	3.91	6.62	0.59
150 ºC	4.30	7.76	0.55

[a] C %: is the subtraction output of carbon content of the composite and pristine HKUST-1. (C %(composite) – C % (blank)).

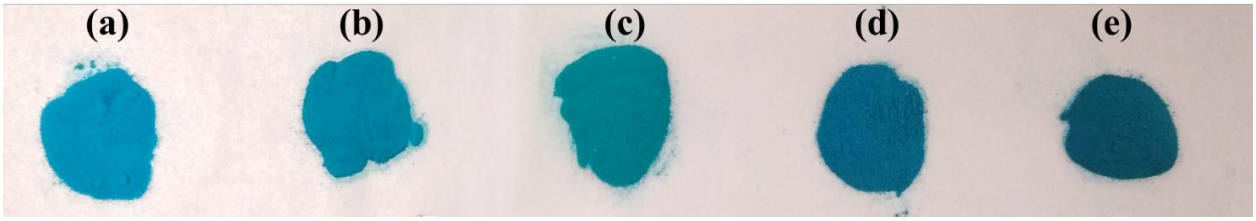

Figure S1. a) Photograph of pristine HKUST-1 and b) composite after loading with CA at 80 ºC for 6 h then polycondensation at c) 90 ºC, d) 120 ºC, and e) 150 ºC for 15 h. (All samples had been kept in air at room temperature for 30 min for equilibrium before taking pictures)

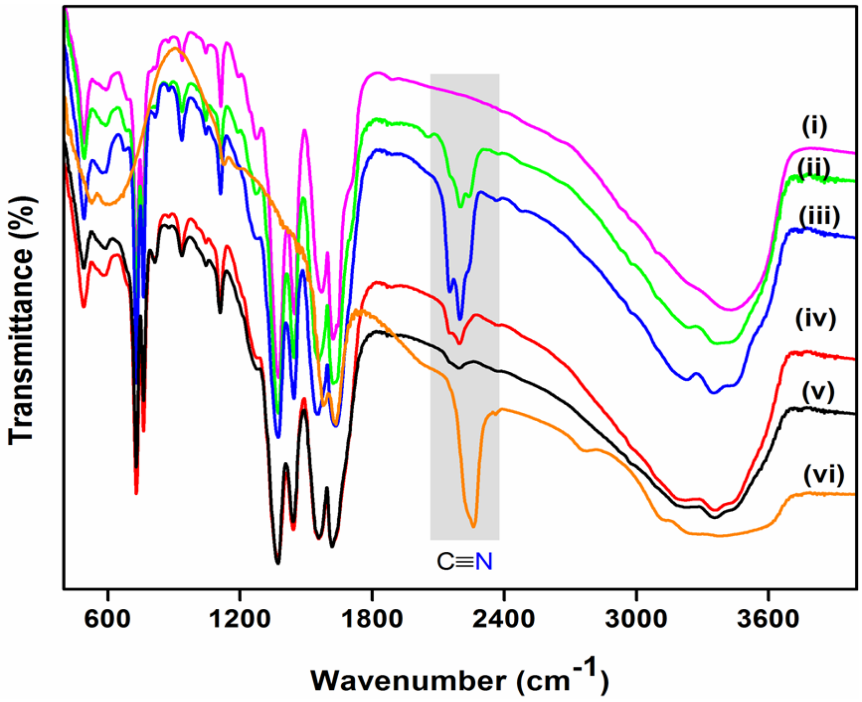

Figure S2. FT-IR full pattern of i) pristine HKUST-1 and composite after loading at ii) 80 ºC for 6 h then polycondensation at iii) 90 ºC, iv) 120 ºC, and v) 150 ºC for 15 h in comparison with vi) CA.

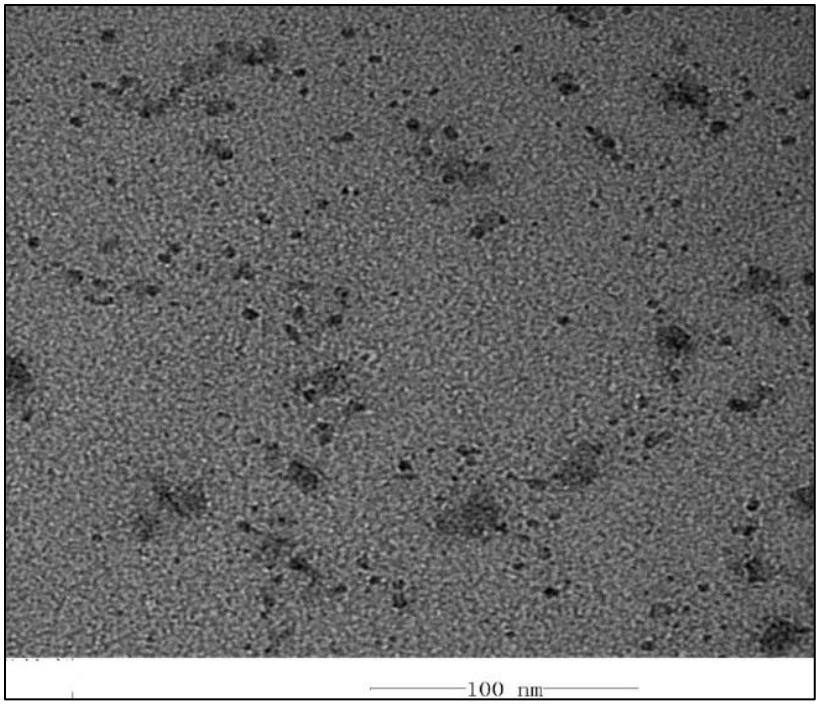

Figure S3. TEM image for g-CNQDs prepared at polycondensation temperature of 150 ºC for 15 h.

The average particle size of g-CNQDs prepared at 150 ºC was calculated to be 3.43 ± 1.82 nm depending on randomly selected 50 particles (avoiding the large aggregates). The larger particle size comparing with the HKUST-1 cavity dimensions could be ascribed to the cavity expansion due to production of ammonia gas as a by-product of the condensation reaction.

2. Reaction time optimization:

Reaction time was optimized by monitoring the condensation of CA at 120 °C every 3 h up to 15 h using FT-IR analysis (Figure S4). The relative intensity of the vibration peaks related to the nitrile group (C≡N) in the range from 2198 to 2245 cm^{-1} had increased after 1 h of the reaction followed by gradual decrease, confirming monomer loading and condensation, simultaneously. It is expected that, CA consumption rate has exceeded the loading rate, leading to gradual decrease in the relative intensity of the vibration peaks. The obvious increase in the N % (Figure S5) confirmed the FT-IR observations and indicated the parallel loading. After 9 h, N % decreased gradually due to condensation and ammonia release. It was noticed that CA vapor has dimerized and solidified inside the reaction vial after 9 h at 120 °C which explain discontinuity of the simultaneous loading. As a result, we extended the condensation period to 15 h to ensure complete maturation of the produced g-CNQDs.

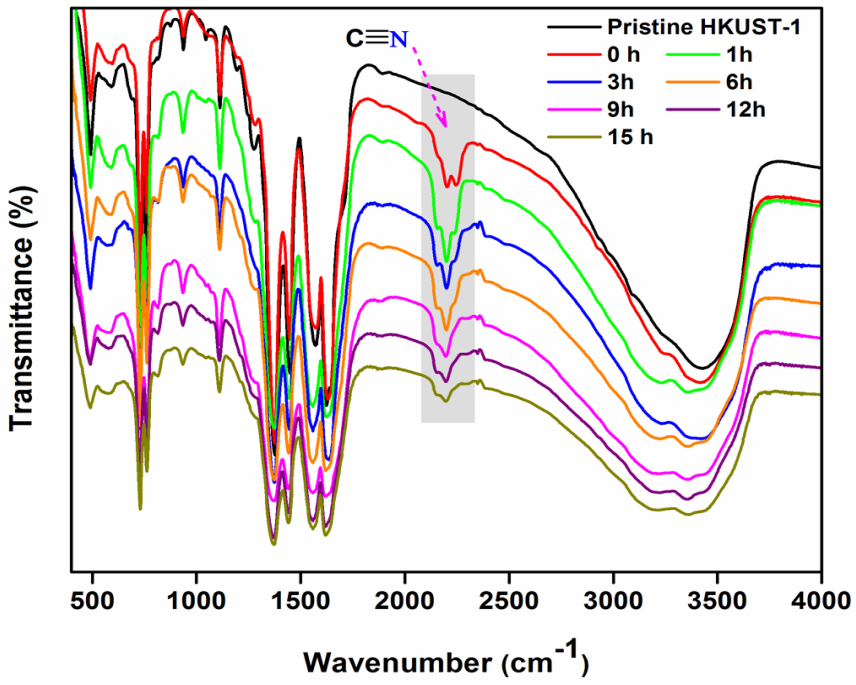

Figure S4. FT-IR spectra of pristine HKUST-1 in comparison with the composites prepared at 120 °C during condensation periods ranged from Zero (HKUST-1 was only loaded with CA for 6h at 80 °C) to 15 h.

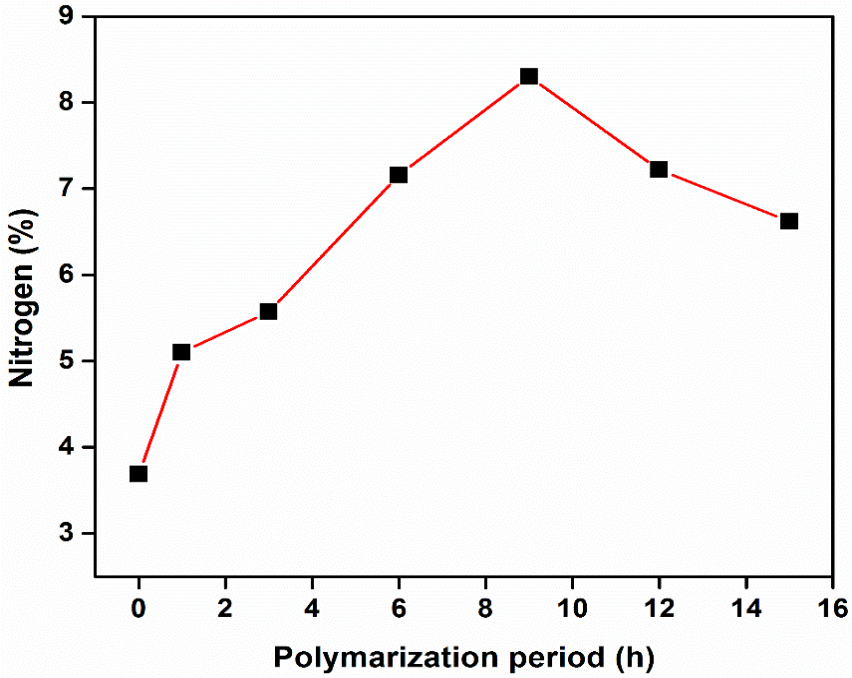

Figure S5. Nitrogen percentage in the composite after loading with CA at 80 ºC/6h then polymerization at 120 ºC during different periods from zero (HKUST-1 was only loaded with CA for 6h at 80 ºC) to 15h.

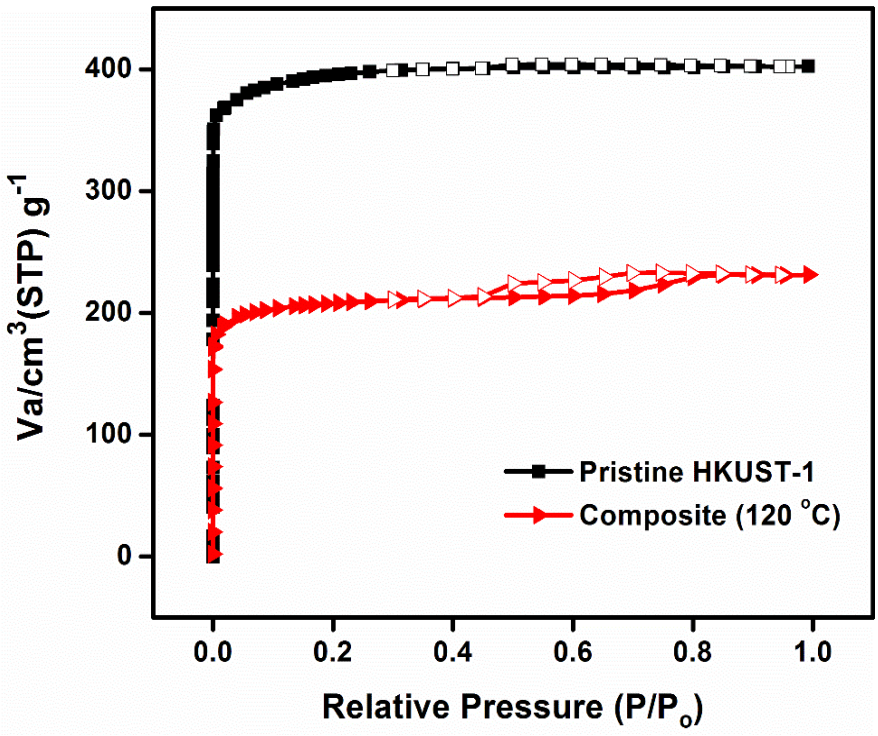

Figure S6. N_2 sorption isotherm at 77 K of pristine HKUST-1 in comparison with the composite prepared at 120 °C/15h.

The N_2 sorption isotherm of the composite prepared at 120 °C showed narrow hysteresis loop that refer to conversion of a small fraction of HKUST-1 micropores into mesopores. This finding could be attributed to inner structure etching caused by ammonia gas produced as a by-product of CA condensation.

3. Control experiment:

The control experiment showed that CA only dimerized into dicyandiamide by heating at 120 ^{o}C for 15 h in absence of HKUST-1 as shown in Figure S7.

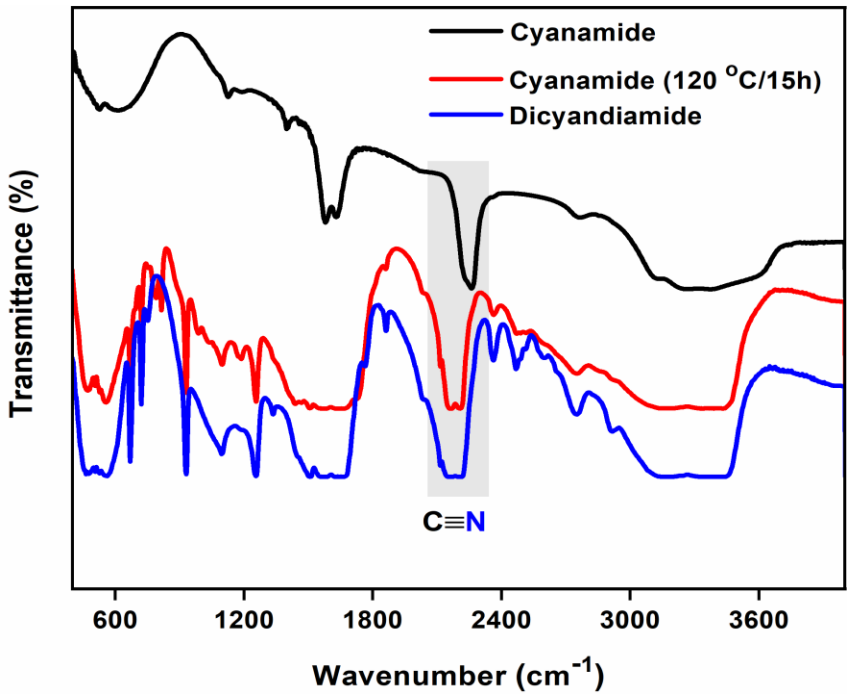

Figure S7. FT-IR patterns of CA before and after heating at 120 ^{o}C for 15 h in comparision with pristane dicyandiamide.

4. Catalytic effect of other copper (II)) forms:

To confirm the role of the copper ion (Cu (II)) in catalyzing the CA polycondensation, other forms of Cu^{2+} were tested like copper acetate and nitrate. The FT-IR patterns of the reaction product (Figure S8) refer to successful production of g-C_3N_4 like material under the same reaction conditions established for production of g-CNQDs inside HKUST-1 cavities. High degree of matching between the FT-IR patterns of the g-C_3N_4 prepared using different copper forms as a catalysts and that produced by thermal condensation at 600 ^oC for 2h was observed. The spectra included sharp absorption peak at 810 cm^{-1} that may be originates from the tri-s-triazine ring-sextant out-of-plane bending vibration confirming the presence of the heptazine rings in the g-CNQDs and bulk g-C_3N_4 structures.[3] The stretching band at 1085 cm^{-1} is related to C-O vibration while the range between 1200 to 1700 cm^{-1} correspond to the vibrations of the C-NH-C or C-N-(C)-C in case of partial or full condensation, respectively.[4] The absorption band from 3000 to 3650 cm^{-1} is primarily attribute to the vibrations of NH_2, NH, and OH groups.[5]

The PXRD patterns (Figure S9) showed one diffraction peak in the range from 27.02^o to 27.40^o originates from the inter-planer stacking of carbon nitride layers confirming the formation of g-C_3N_4 under the established mild conditions depending on the catalytic effect of the Cu (II) ions whether in the HKUST-1 framework or in simple copper forms like acetate or nitrate.[6]

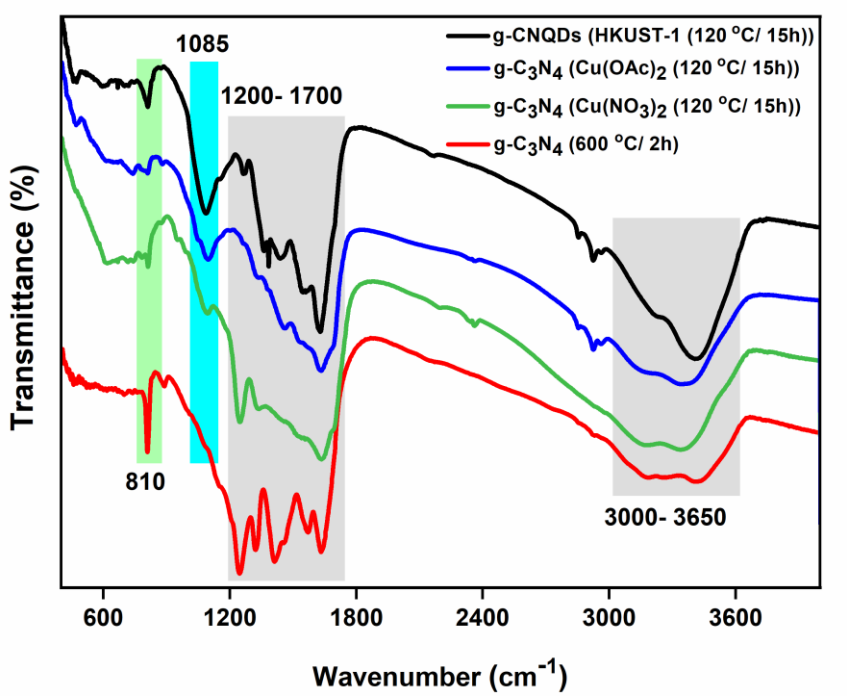

Figure S8. FT-IR spectra of graphitic carbon nitride produced by catalytic polycondensation of CA using copper in three different chemical forms ($Cu_3(BTC)_2$ (HKUST-1), $Cu(OAc)_2$, and $Cu(NO_3)_2$) in comparition with that produced by thermal condensation at 600 °C for 2h.

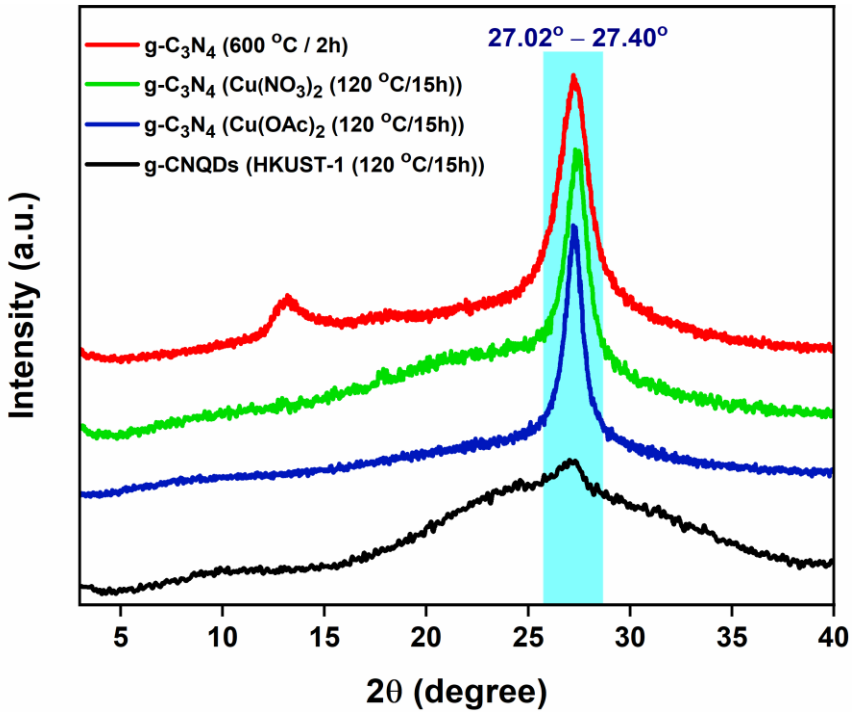

Figure S9. PXRD pattern of graphitic carbon nitride produced by catalytic polycondensation of CA using copper in three different chemical forms ($Cu_3(BTC)_2$ (HKUST-1), $Cu(OAc)_2$, and $Cu(NO_3)_2$) in comparition with that produced by thermal condensation at 600 °C for 2h.

5. NMR analysis for the organic linker (BTC) after the catalytic condensation of CA at 150 °C/15h:

Because CA is a strong nucleophile, we suspect that, it could attack the carboxylic group of the organic lanker in HKUST-1 skeleton as a side reaction. To exclude this doubt, the ligand was analyzed by ^{1}H- and ^{13}C-NMR after composite (prepared at 150 °C/15h) digestion in acidic medium (Figure S10). The obtained patterns had completely matched with that of the pure trimesic acid, which reveals that no side reactions happened at the condensation temperature.

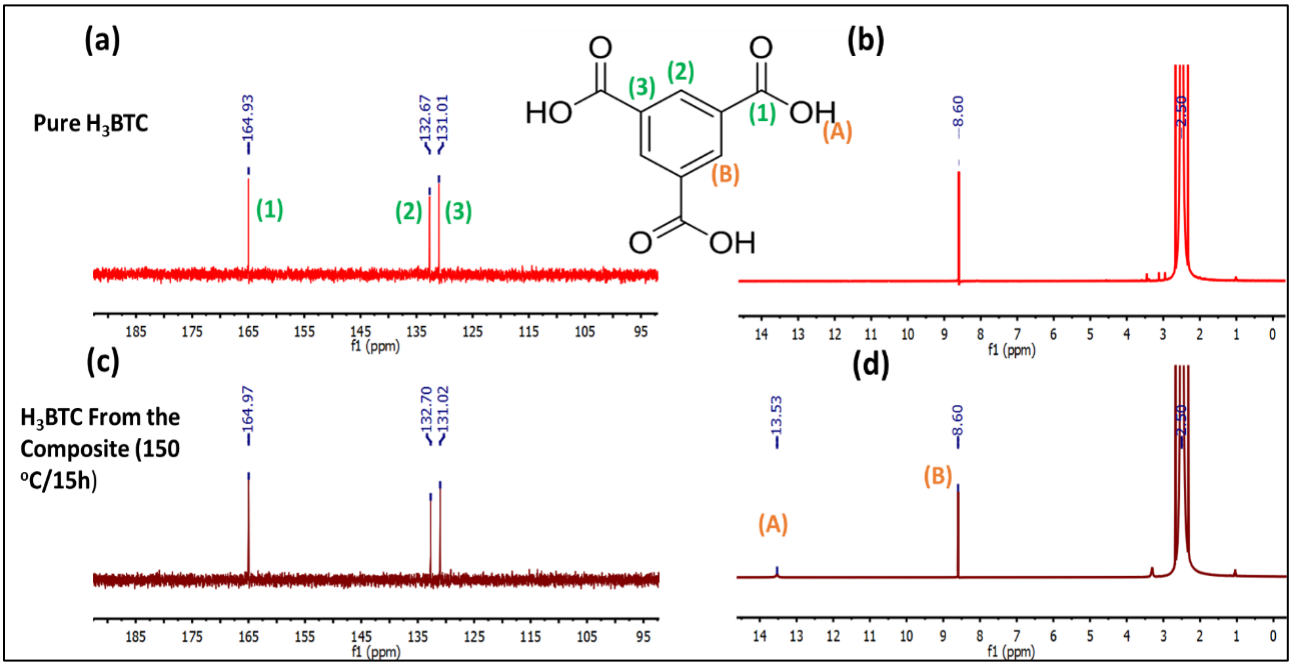

Figure S10. a) and c) ^{13}C-NMR and b) and d) ^{1}H-NMR of pure 1,3,5-benzene tricarboxylic acid (H_3BTC) and that collected from g-CNQDs@HKUST-1 composite prepared at 150 °C/15 h.

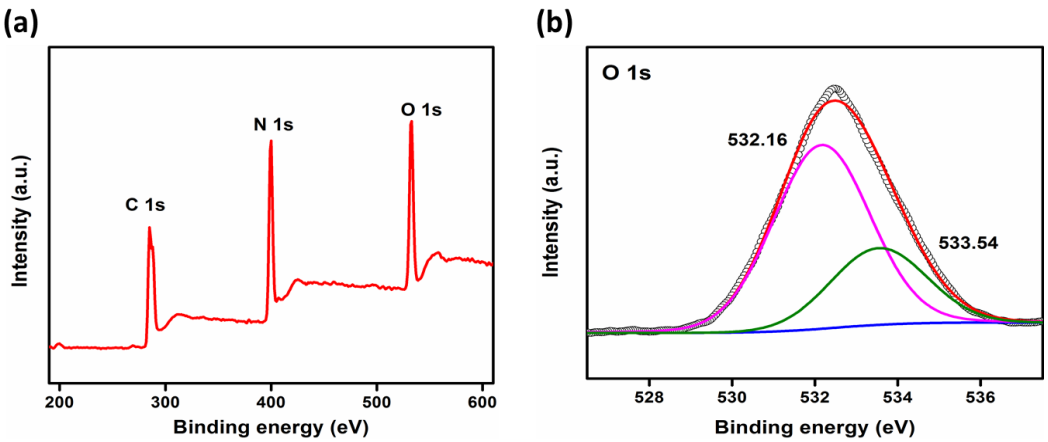

Figure S11. a) X-ray photoelectron spectroscopy survey and b) deconvoluted O 1s spectrum for the produced g-CNQDs.

The XPS survey of the as prepared g-CNQDs included three peaks at binding energies of 284.80, 399.47 and 532.47 eV related to carbon, nitrogen, and oxygen, respectively as shown in Figure S11a.[7] The O 1s broad band (Figure S11b) had been deconvoluted into two peaks at 532.16 and 533.54 eV that may be relate to C-O and C=O, respectively.[8] Presence of oxygen in the structure of the g-CNQDs might be due to surface oxidation during cleanup and removal of adsorbed copper ions using nitric acid (2 M) at room temperature for 2 h. Another source is the carbon dioxide adsorbed on the surface of the QDs. As shown by the XPS, g-CNQDs contain three kinds of nitrogen atoms that could attract carbon dioxide to the surface of the QDs. Presence of C=O in the composition of the g-CNQDs has been detected by the XPS as this technique characterize only the surface layer of the material. FT-IR did not show the vibrations related to this group. Oxygen species on quantum dot surface is a general phenomenon because of its high surface energy and thus affinity to oxygen-containing species, like CO_2, H_2O etc., in air.

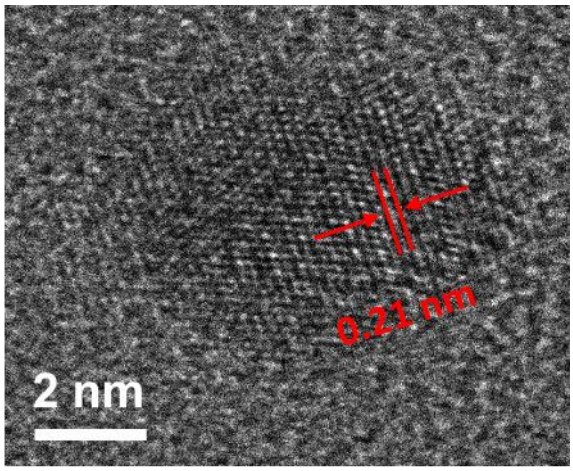

Figure S12. HRTEM image showing the lattice planes of g-CNQDs with lattice spacing of 0.21 nm.

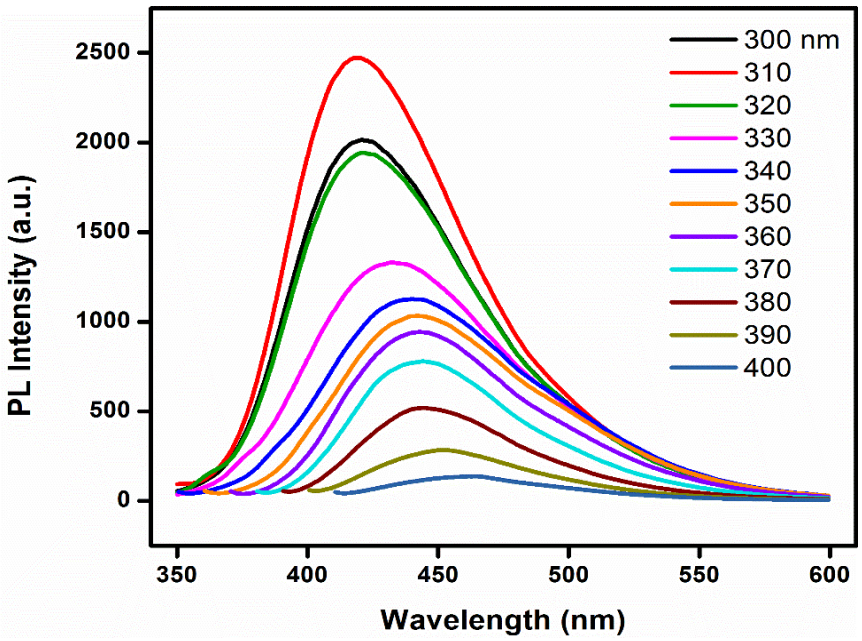

Figure S13. g-CNQDs photoluminescence at different excitation wavelengths (λ_{ex}) from 300 to 400 nm.

6. Effect of pH on the PL intensity of the g-CNQDs.

The pH effect on PL intensity was examined in the range from 1 to 14 (Figure S14). It was observed that, PL intensity is sensitive to the pH of the medium, where the highest PL intensities were recorded in the range from 7 to 12. While below and above this range quenching could happen. The pH dependent PL phenomenon was ascribed to the interaction between the electron lone pair (LP) of N atom and the surrounding ions in the medium. For example, in acidic medium protons will interact with the LP and prevent the electron transition between the LP valance band and the π* conduction band that will partially deactivate the PL emission.[9]

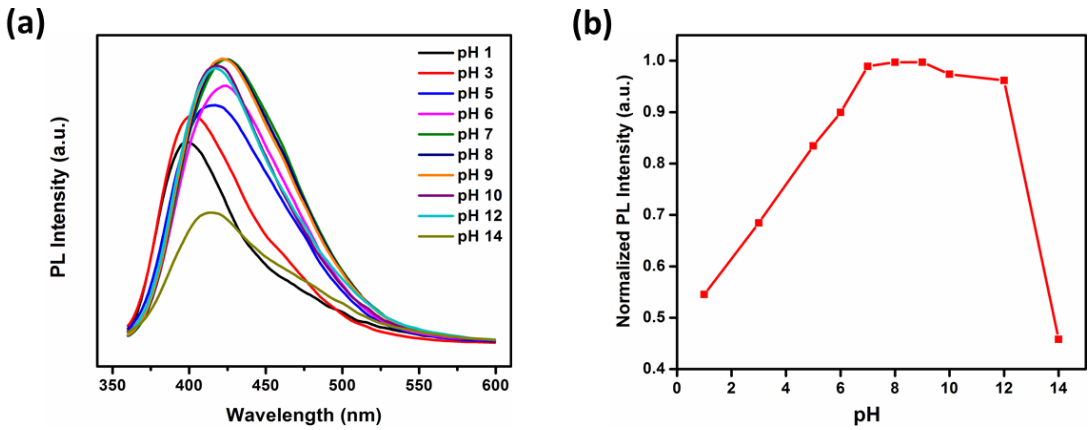

Figure S14: a) pH effect on the PL intensity of the g-CNQDs; b) the relation between the pH and the normalized PL intensity at 420 nm.

7. Zeta potential of the g-CNQDs at different pH values:

The prepared g-CNQDs surface was found to be negatively charged at pH 7 with zeta potential equal to – 5.74 mV. Changing the pH value to 4 led to neutral to positively charged QDs with zeta potential value of 0.31 mV (Figure S15).

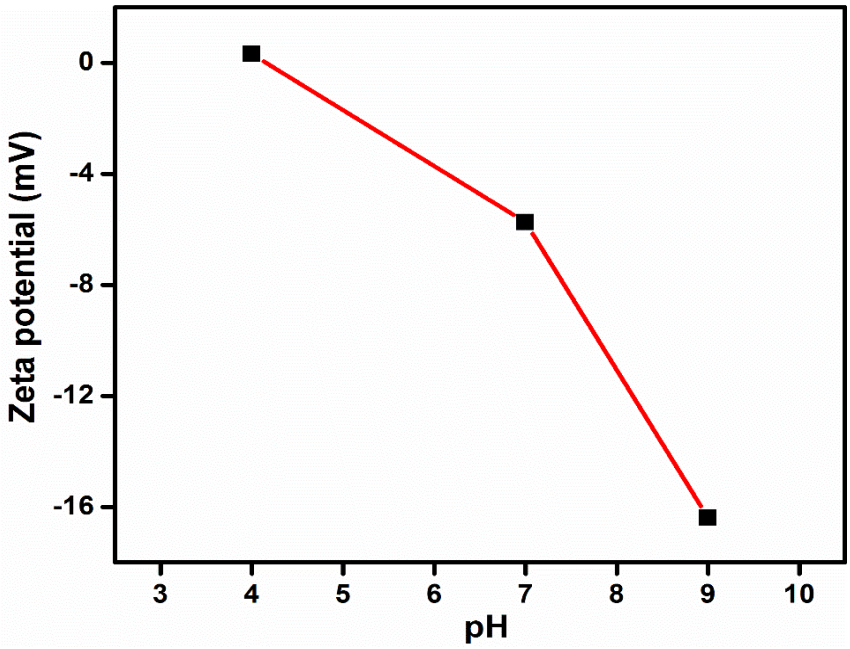

Figure S15. Zeta potential of g-CNQDs dispersed in buffer solution versus the pH of the medium.

8. Quantum Yield Measurements:

The quantum yield (QY) of g-CNQDs was calculated by comparing the integrated PL intensities (excitation at 310 nm) and absorbance values (at 310 nm) of the quinine sulfate in 0.1 M H_2SO_4 as a reference (Φ = 0.54) and g-CNQDs in water (Figure S16). A series of concentrations for g-CNQDs and quinine sulfate standard were prepared so that the absorbance was less than 0.1 at the selected excitation wavelength to avoid self-quenching. The QY was calculated according to equation (1):[10]

$$\Phi_X = \Phi_{ST} \times (m_X/m_{ST}) \times (\eta^2_X / \eta^2_{ST}) \qquad (1)$$

where, Φ is the quantum yield, m is the plot slope, and η is the solvent refractive index (η = 1.33). The subscript X and ST refer to the g-CNQDs and quinine sulfate, respectively. The calculated QY was found to be 3.1 %

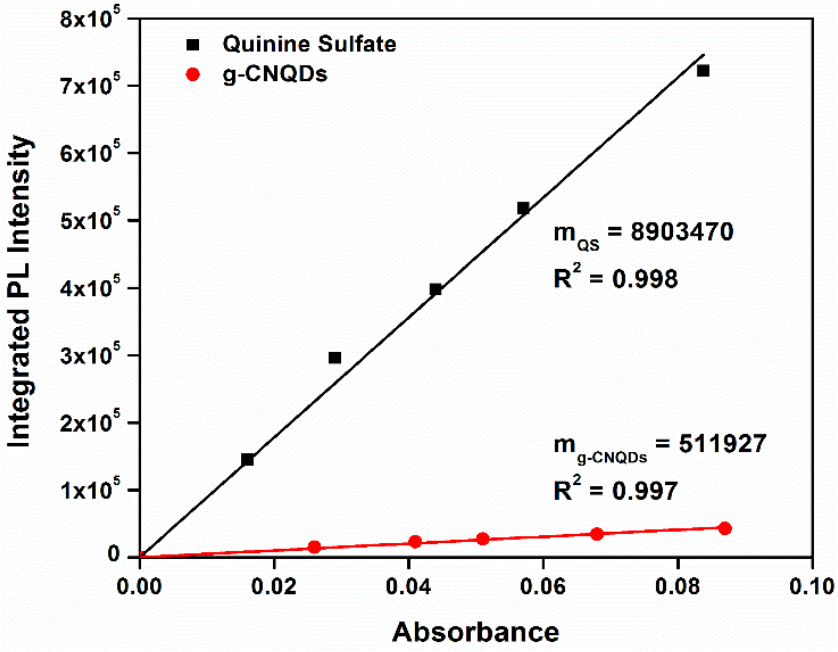

Figure S16. Linear relation between the integrated PL intensity and absorbance of the quinine sulfate as a standard and prepared g-CNQDs.

References:

[S1] K. Schlichte, T. Kratzke, S. Kaskel, *Microporous. Mesoporous. Mater.* **2004**, *73*, 81–88.

[S2] H. K. Kim, W. S. Yun, M. -B. Kim, J. Y. Kim, Y. -S. Bae, J. Lee, N. C. A. Jeong, *J. Am. Chem. Soc.* **2015**, *137*, 10009–10015.

[S3] Y. Wang, Y. Li, W. Ju, J. Wang, H. Yao, L. Zhang, J. Wang, Z. Li, *Carbon* **2016**, *102*, 477 – 486.

[S4] a) Y. Wang, J. Wang, P. Ma, H. Yao, L. Zhang, Z. Li, *New J.Chem*. **2017**, *41*, 14918 – 4923; b) H. Wang, S. Jiang, S. Chen, D. Li, X. Zhang, W. Shao, X. Sun, J. Xie, Z. Zhao, Q. Zhang, Y. Tian, Y. Xie, *Adv. Mater*. **2016**, *28*, 6940 – 6945; c) T. Malina, K. Poláková, J. Skopalík, V. Milotová, K. Holá, M. Havrdová, K. B. Tománková, V. Čmiel, L. Šefc, R. Zbořil, *Carbon* **2019**, *152*, 434 – 443.

[S5] Y. Yin, Y. Zhang, T. Gao, T. Yao, J. Han, Z. Han, Z. Zhang, Q. Wu, B. Song, *Mater. Chem. Phys*. **2017**, *194*, 293 – 301.

[S6] P. Niu, L. Zhang, G. Liu, H.-M. Cheng, *Adv. Funct. Mater*. **2012**, *22*, 4763 – 4770.

[S7] M. Rong, L. Lin, X. Song, T. Zhao, Y. Zhong, J. Yan, Y. Wang, X. Chen, *Anal. Chem*. **2015**, *87*, 1288 – 1296.

[S8] a) Y. Zhan, Z. Liu, Q. Liu, D. Huang, Y. Wei, Y. Hu, X. Liana, C. Hu, *New J. Chem.* **2017**, *41*, 3930–3938.

[S9] Z. Song, T. Lin, L. Lin, S. Lin, F. Fu, X. Wang, L. Guo, *Angew. Chem. Int. Ed*. **2016**, *55*, 2773 –2777; *Angew. Chem*. **2016**, *128*, 2823– 2827.

[S10] J. Zhou, C. Booker, R. Li, X. Zhou, T.-K. Sham, X. Sun, Z. Ding, *J. Am. Chem. Soc.* **2007**, *129*, 744–745.